International Journal of Engineering and Advanced Technology (IJEAT)
ISSN: 2249-8958 (Online), Volume-8 Issue-5, June 2019

Wavelet-Based Automated DNA Sizing of Fragments through AFM Image Processing

S. Anand, B.Lakshmanan, J. Murugachandravel, K. Valarmathi, Abhisha Mano, N. Kavitha

Abstract: ***Atomic Force Microscope (AFM) is a procedure to investigate the size of the DNA fragments. In this paper, an algorithm is presented to determine the DNA fragment size from images of DNA molecules. The previous automated approach that uses conventional filters fails to have multidirectional and multiscale properties. This automated approach implements an algorithm on multiscale shift invariant wavelet decomposition to recover the DNA fragments. In order to avoid erroneously evaluated fragments, this algorithm also includes thinning and threshold process on Euclidean norm of wavelet decomposition. The Euclidean norm of multilevel decomposition is able to control the noise whereas the hysteresis threshold ensures proper connectivity. Computer generated and real images are tested for different fragment size in various noise background. The DNA sizing of fragments is compared with already existing method. The improved performances are analyzed using Figure of Merit, accuracy, sensitivity, specificity and false positive rate.***

Index Terms: ***AFM image, DNA Fragments, Wavelet Transform, DNA sizing.***

I. INTRODUCTION

DNA provides important information of DNA fragments. The contour length of DNA fragments determined by Atomic Force Microscopy (AFM) is a widely used tool for investigating the physical properties. The length of a DNA fragment can be used to infer the helical rise [1] interactions, and mixtures [2] (i.e.) ligand binds [1, 2]. Characterization of a DNA molecule through fragment length and the molecule profile is possible [3]. DNA sizing through Gel electrophoresis methods is very common. Low speed (i.e.) high processing time and requirement of large amount of DNA samples are the limitations of these methods. Light microscopy is another approach to compute the length of the DNA which is stained [4, 5]. DNA line are traced through the edge points and thinned by 8-connectivity method [6]. There are many methods [7-11] to process the AFM images to compute length using a set of image processing steps and they are not utilizing the multiple scale representation of the images. The automated algorithm uses single threshold and affected by inaccuracy and the presence of noise. In [3] an image processing based method is developed to fragment the points that provide better accuracy than previous methods. They used points pruning, molecule removing, and length computation are some of the image processing steps. The above algorithms use only linear filters for DNA sizing through image processing and fail to achieve the multi scale and multidirectional information embedded in AFM DNA images. In addition, fragments information is lost due to application of smoothing filter to remove the background noise. The DNA and other nucleic acids under physiological conditions is analyzed by using AFM in nanometer scale resolution. The technique has been used to study the structure of nucleic acids such as super coiled, kinked, and looped DNA and DNA protein complexes [12]. Wavelet transform (WT) is an evolving technology, which offers far higher degrees of information processing compared to standard transforms. This paper proposes, WT based approach to provide sizing the DNA fragments. WT have more flexible tool compare with other time-frequency analysis. It is possible due to property that time scale width of the WT window stretched to original signal characteristics both in scale and time, especially in image processing applications. This makes it particularly useful for analyzing the images in multi scale and multi direction [13]. WT method is sometimes referred to as a "mathematical magnifier" due to its ability to insights the multi-scale and multidirectional characteristics of DNA fragments and inform about these characteristics. Contribution of this work is to develop a wavelet based DNA sizing algorithm using multidirectional and multi scale property of WT. This image processing algorithm composed of SWT, non-maximal suppression of fragments pixels, hysteresis threshold followed by thinning to provide higher accuracy than previous solutions. Also, it avoids errors occurred in the dynamic structure and intrinsic curvature which is very commonly found in DNA.

II. METHODS AND MATERIALS

To construct the physical genome maps and genotyping, fragment points from DNA through AFM image provides essential information. Generally, the DNA sample is prepared by dissolving DNA solution in buffer agent, which contains HEPES (hydroxyethyl piperazineethanesulfonic acid), and Nickel (II) chloride.

Manuscript published on 30 June 2019.
* Correspondence Author (s)
S Anand, Professor, Department of ECE, Mepco Schlenk Engineering College, Sivakasi, India
B.Lakshmanan, Asst. Professor (Sr. Grade), Department of CSE, Mepco Schlenk Engineering College, Sivakasi, India
J.Murugachandravel, Asst. Professor (Sl. Grade), Department of MCA, Mepco Schlenk Engineering College, Sivakasi, India
K.Valarmathi, Senior Lecturer, Department of ECE, S.Vellaichamy Nadar Polytechnic College, Virudhunagar, India
Abhisha Mano, Asst. Professor, Department of ECE, Rajas International Institute of Technology for Women, Nagercoil, India
N.Kavitha, Assistant Professor, Department of CSE, Saranathan Engineering College, Tiruchirapalli, India

A drop of this prepared solution with concentration of 1mg/ml is placed in a mica substrate. After incubation for five minutes, the prepared DNA sample is placed in the AFM for scanning. The AFM scans of DNA sample are stored as image for further processing and applications.

From the obtained AFM DNA image, the fragments of DNA are identified using 8- connectivity. However, determining the fragments from the AFM images is not an easy task due to reasons like (i) While capturing itself noise is added with the original (ii) All pixels do not have perfect 8 connectivity (iii) While preprocessing some of the valid/invalid pixels are converted into invalid/valid pixels. In order to recover fragments, image-processing operations are performed on not only the pixels corresponds to fragments, but also the valid neighboring pixel. However, for extracting the accurate fragment point and increase accuracy, thinning process is applied. Although this process is efficient, small part of spurious branches will appear and pruning is used to remove it. Pruning not only removes spurious branches but also the critical molecules. In addition, AFM images contain noise that have to be removed by preprocessing such as filtering and threshold. In [3] authors implemented an automatic method to size the fragments from AFM DNA images uses conventional filters. The effectiveness of multi resolution transforms over the conventional filters in image processing is well known. The following section gives the intuition of wavelets in fragment recovery.

A. Wavelet Transform in DNA fragment recovery

The WT is a powerful tool for image analysis. The image representation in terms of frequency and local spatial regions over a various scales provides an excellent for image features analysis. Since our interest is the fragment recovery from AFM DNA images and in which DNA fragments have simple features in different size and scales often be characterized in frequency domains. WT is a perfect tool to detect discontinuities, and periodicities on an image. More than this, the WT is capable to represent time and scale information of a signal into multiple resolutions and scales, and act as a mathematical insight to inspect and inform about the significant features. The following section explains the DNA fragments in an AFM image and its representation in the wavelet domain along with its recovery. Let us consider a two dimensional (2D) AFM DNA image $f(x,y)$ and smoothing function $\theta(x,y)$ and $\theta(x,y)$ satisfies $\iint \theta(x,y)\,dx\,dy = 1$. Now, the image $f(x,y)$ can be smoothed and described as $(f * \theta_s)(x,y) = \iint f(x-u, y-v)\theta_s(u,v)\,dudv$. Where $\theta_x(u,v) = \frac{1}{s^2}\theta(\frac{u}{s},\frac{v}{s})$, and $s > 0$ stands for a smoothing scale. Naturally, fragments in an AFM DNA image has high background to foreground ratio and located in high gray level transitions. Determining the derivative components is the best way to detect gray level transitions which will imply fragments. When we calculate the derivative of f(x,y) to detect location of the fragments, their orientation also important. At each pixel, derivative reaches maximum along the gradient direction within a window, and can be represented by $\text{grad}(f * \theta_s)(x,y) = i\frac{\partial}{\partial x}(f * \theta_s)(x,y) + j\frac{\partial}{\partial y}(f * \theta_s)(x,y)$. Where i and j correspond to x-axis and y-axis respectively. In order to detect the fragments in DNA image, the local modulus maxima of WT can be considered. The modulus maxima reaches maximum along with the gradient direction for a given window.

$$|\text{Grad}(f * \theta_s)(x,y)| = \left(\left|\frac{\partial}{\partial x}(f * \theta_s)(x,y)\right|^2 + \left|\frac{\partial}{\partial y}(f * \theta_s)(x,y)\right|^2\right)^{0.5}$$

These maximum modulus locations will become the features of DNA fragments. Also, $\Psi^1(x,y) = \frac{\partial\theta}{\partial x}(x,y)$, $\Psi^2(x,y) = \frac{\partial\theta}{\partial y}(x,y)$ where $\Psi^1(x,y)$ and $\Psi^2(x,y)$ become 2D wavelets. It is easy to know that $|\text{grad}(f * \theta_s)(x,y)| = \frac{1}{s}\left(\left|W_s^{\Psi^1} f(x,y)\right|^2 + \left|W_s^{\Psi^2} f(x,y)\right|^2\right)^{0.5}$ T

The modulus maxima of WT of a given image f(x,y) can be described as

$$M_s f(x,y) = \left(\left|W_s^{\Psi^1} f(x,y)\right|^2 + \left|W_s^{\Psi^2} f(x,y)\right|^2\right)^{0.5}. \quad (1)$$

It is clear that $|\text{grad}(f * \theta_s)(x,y)| = \frac{1}{s}M_s f(x,y)$. Mathematically, an edge is a class of 1D or 2D singularity which can be analyzed through Lipschitz exponent. An edge can be categorized into roof, dirac, and step. Based on the nature of DNA fragments in AFM image, they belong to step edge. The ideal step edge is $e(x) = \begin{cases} 1, & x \geq x_0 \\ 0, & x < x_0 \end{cases}$ at location x_0.

Let $L^2(R)$ be a Hilbert space of square integral functions on R, and $\Psi \in L^2(R)$ be a WT basis function, (i.e.), $\Psi(x)$ decreases fast when 'x' goes to infinity and satisfies $\int \Psi(x)dx = 0$. In edge detection, the smoothness of $\Psi(x)$ affects the results of location of the detection. Usually, more smoothness better (less noise) is the result. A compactly supported Haar WT function is chosen as $\Psi(x)$. $\forall f(x) \in L^2(R)$ and $s > 0$, the WT of f(x) with the scale 's' is defined as $W_s f(x) = (f * \Psi_s)(x) = \int f(t)\frac{1}{s}\left(\frac{x-t}{s}\right)dt\,\Psi$, Where '$*$' denotes the function convolution, and $\Psi_s(x) = \frac{1}{s}\Psi\left(\frac{x}{s}\right)$. Particularly, $W_{2j}\,f(x), (j \in z)$ is called dyadic WT, with 'z' set of integers. The WT of a step edge is described by $W_s e(x) = \int_{-\infty}^{-|x-x_0|s^{-1}} \Psi(t)dt$. Particularly, at point x_0, the wavelet transforms of these basic edge structures become

$$W_s e(x_0) = -\int_0^{\infty} \Psi(t)dt \quad \text{if } x_0 \text{ is a step edge} \quad (2)$$

B. Proposed Method of DNA fragment recovery

The functional block diagram Fig.1 overviews the basic steps of our algorithms.

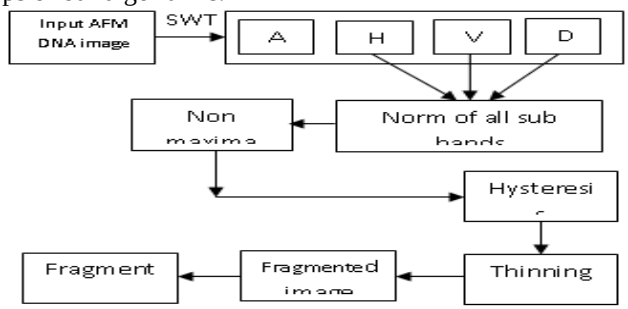

Figure 1 Block Diagram Proposed Algorithm

Published By:
Blue Eyes Intelligence Engineering
& Sciences Publication (BEIESP)

From Eq.1, it is understand that the WT $W_s e(x_0)$ of the step edge is a nonzero and constant that is independent on the scale of the WT. The sign at both sides of the neighborhood of x_0 and the extreme is reached at x_0. Since the WT of the edges are independent, the ability to detect edges in three directions is affordable. Step-structure edge scales are independent it is devoted to edge structure. Due to following reasons, these are important to our applications. The edge is not an ideal one and the image is distorted by noise along with small error in the background Before applying the WT on the AFM DNA image, the input image is converted into gray level image. Since the image is a set of discrete data, Discrete Wavelet Transform (DWT) is used. However, the classical DWT suffers a drawback, (i.e.) time varying transform. Stationary Wavelet Transform (SWT) is alternate to DWT to achieve the invariance property. The output of each stage (level) of SWT has the same size (i.e.) number of feature samples as input. This most useful property is utilized for our breakdown point's detection. The SWT is very simple and is close to the DWT except down sample. More precisely, SWT is obtained by convolving the image with the high and low pass filters as in the DWT but without reducing the number of samples. For images, an algorithm similar to the 1D case is possible for 2D wavelets and scaling functions obtained from 1D ones by tensor product.

C. Determination of fragments from SWT decomposition

The sub bands that are obtained from the SWT decomposition needs to combined to determine the DNA fragments in the AFM images. This step consisting of two significant processes to (i) Collect the fragments and (ii) Control the noise. In order to collect all the fragments from various scales, the sub bands of each scale is added and thereby, the multi scale and multi directional SWT decomposition that represents the effective fragments are collected. In order to control the noise, scale multiplication technique is used [14, 15]. Instead, this paper uses Eq. 3.to collect the all the fragments with effective noise control.

$$M_s f(x,y) = \prod_{s=1}^{N} \left\{ \sum_{\theta=1}^{3} \left| W_s^{\Psi^\theta} f(x,y) \right|^2 \right\}^{\frac{1}{2}} \qquad (3)$$

D. Non-maximal suppression

The edge magnitude M(x,y) may contain multiple responses (ridges) about the local maxima. Non-maxima suppression removes the pixels upholding 8 connectivity contours and thins wide contours in DNA fragments. If the edge is in the north and south direction (zero degree gradient angles) the pixel will be the edge while the gradient magnitude is larger than the west and east directional magnitudes. In practice, either all or all but one is suppressed according to some ordering. The second step of keeping the 8 connectivity (non maxima suppression) makes the gradient magnitude at a pixel zero if it is smaller than the gradient magnitude at any of the two pixels in the direction of quantized gradient. For example, if the quantized gradient direction is horizontal, then the gradient magnitude values are compared with its right and left, and make smaller values to zero.

E. Hysteresis threshold

After the non-maxima suppressed (NMS) operation, the outputs still contains noisy and local maxima. The fragments strength may be changed in various points of the contour. A threshold of M(x, y) is needed to remove these weak and noisy edges while preserving the 8 connectivity. Hysteresis threshold is applied to the NMS output. The hysteresis threshold algorithm uses two thresholds, T_{high} and T_{low}. A pixel (x, y) is called strong if $NMS(x, y) \geq T_{high}$. A pixel (x, y) is called weak if $NMS(x, y) < T_{low}$. Discard the pixel (x, y) if it is weak with respect to (x, y); if it is strong output the pixel. For a correct candidate, apply the 8 connected local maxima along the edge, and $NMS(x, y) > T_{low}$. A tracking algorithm starting from pixels above the high threshold and stopping pixels below the low threshold finds the edges.

F. Thinning and Size calculation

To attain a good tradeoff between accurate molecular profile and execution time, each point in the fragments match with a set of masks and match points are deleted and it ends when no more variations are detected in the image. In order to find the size of fragments first we must use 8-connectivity. Using 8-connectivity, we can find how much number of connected fragments and total fragment size. The fragment size thus determined in term of pixels is converted into nanometer with the help of conversion table.

III. Experimental Results

The proposed algorithm is implemented using Matlab 7.8 and we obtain the eight real AFM DNA images as shown in Fig.2 to qualitatively evaluate the proposed algorithm. The performances are compared to a method described in [3].

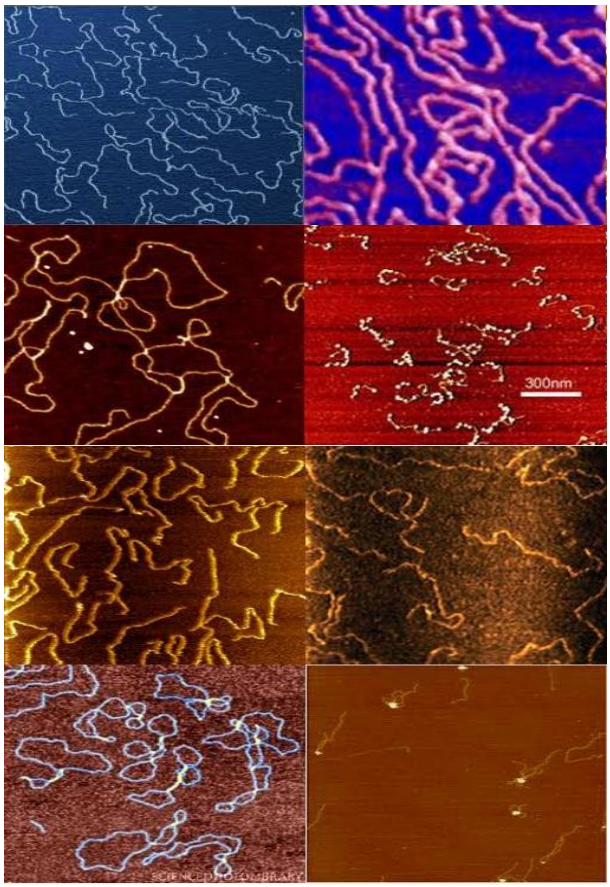

Figure 2 Testing images:'DNAimage1' to 'to 'DNAimage8'

Published By:
Blue Eyes Intelligence Engineering
& Sciences Publication (BEIESP)

In order to implement the WT decomposition of testing images SWT is applied. This paper uses 'Haar' wavelet and its high pass and low pass coefficients are given by [-0.703 0.703] and [0.703 0.703]. Since the SWT is a shift invariant WT and without sub sampling process,

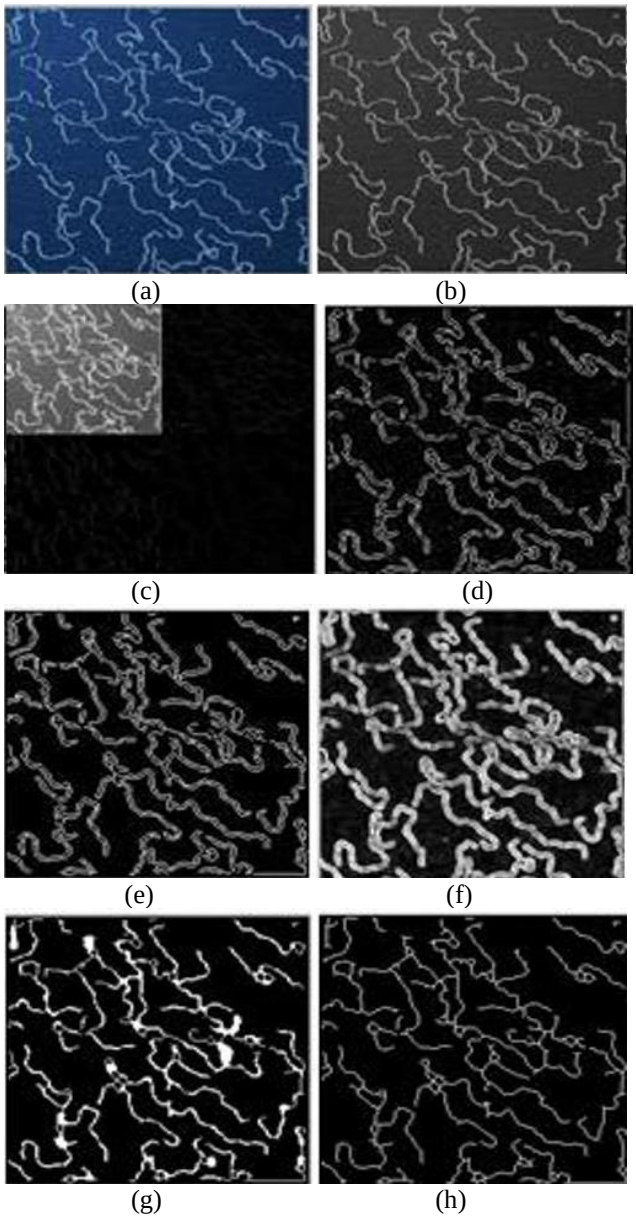

Figure 3 Various step results of proposed method (a) Input 'DNAimage1', (b) RGB to Gray Conversion, (c) Level 1 Sub band Decomposition of Stationary Wavelet Transform of (a), (d) Modulus Maxima of WT decomposition (e) Suppression of non-maximum points, (f) Hysteresis threshold Applying on (e),(g) Morphological thinning of (f), (h) fragmented image.

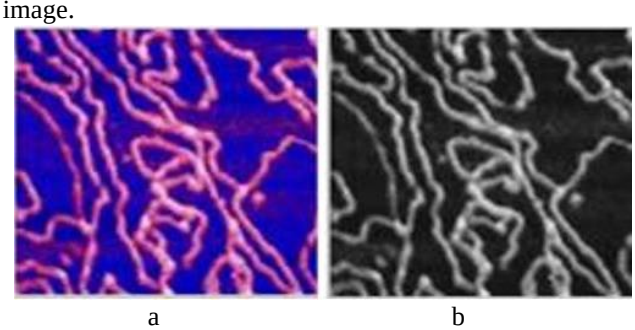

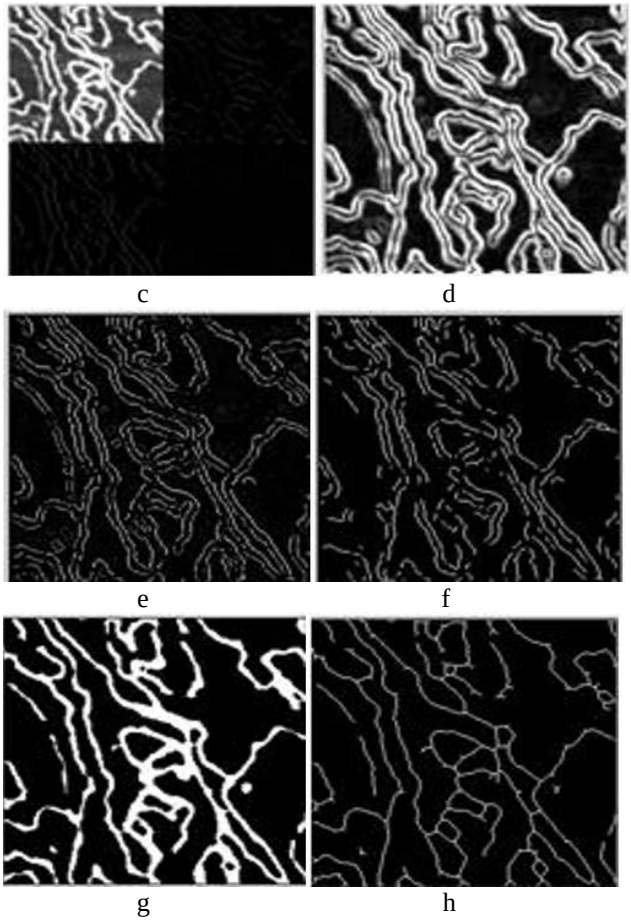

Figure 4 Various step results of proposed method (a) Input

'DNAimage2', (b) RGB to Gray Conversion, (c) Level 1 Sub band Decomposition of Stationary Wavelet Transform of (a), (d) Modulus Maxima of WT decomposition (e) Suppression of non-maximum points, (f) Hysteresis threshold Applying on (e), (g) Morphological thinning of (f), (h) fragmented image. the sub bands are equal in size. The decomposed sub bands represent the various directional features that are combined by using Eq.3 to provide complete DNA fragments. Due to multiple responses, the magnitude M(x, y) of fragments may contain wide ridges around the local maxima and non-maxima suppression operation is performed. It removes the NMS pixels and maintaining the 8 connectivity property of the fragment contours. The various steps of the proposed algorithm are described in the Fig 3 and Fig 4. Fig 3(a) shows the original image and Fig 3(b) shows the color to gray converted image. Fig 3(c) depicts the one level sub band decomposition of Fig 3(b) using 'Haar' wavelet. The technical advantage of the Haar wavelet is that symmetrical as well as orthogonal and helpful in fragment determination. This property is the benefit for the analysis of images with sudden transitions. In order to implement SWT algorithm for image processing, this paper uses a two dimension version of the wavelet filter banks.

Published By:
Blue Eyes Intelligence Engineering
& Sciences Publication (BEIESP)

In the two dimension case, the one dimension wavelet filter bank is applied to the rows of the image. After applying the two dimension filter to each row of given image in the form of matrix, two sub band images are obtained.

While applying 1 dimension filter to each column of both the two sub band images, four images such as approximation band (A), horizontal band (H), vertical band (V) and diagonal band (D) images are obtained. The oriented fragments are shown in Fig 4 (c). The next step of algorithm is NMS and hysteresis threshold. The illustrated example uses lower and upper threshold as 0.1 and 0.4 respectively. After hysteresis threshold, we apply morphological thinning operation on the threshold image to proper identification of the fragments, which fulfill the 8 connectivity. Since WT have variety of wavelet families, the algorithm is tested with 'Haar' and Daubechis' wavelets, and all among 'Haar' provides best results. In addition, the algorithm is tested on various resolution levels. While implementing SWT at resolution level 3 of 'Haar' the fragments were completely lost whereas implementing SWT at 'level 5' of 'db1' many spurious fragments were added. In addition, while implementing wavelet transform at 'level 4' of 'db2' the actual fragments were broken. Hence, we obtained the best result at SWT 'level 4' of 'db1'. The fragments recovered for various levels and wavelet types are illustrated in Fig.5.

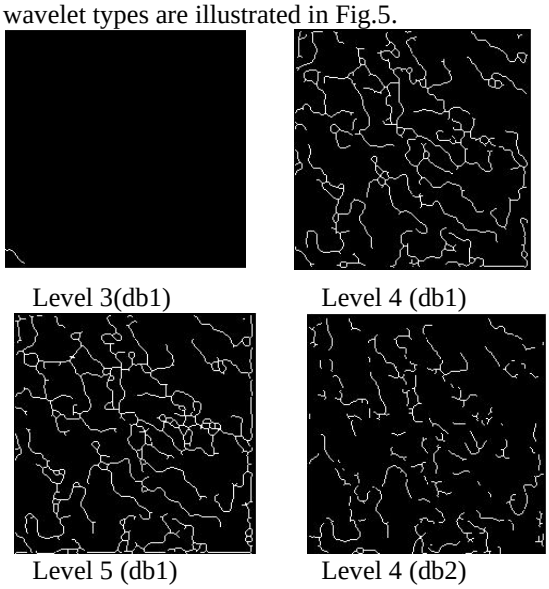

Figure 5: Algorithm outputs of various wavelets and different levels

IV. PERFORMANCE EVALUATION

This paper considers eight real images and six computer simulated images to estimate the performance of this developed algorithm. The real images are chosen in such a way that the images have different sizes, different background colors, and varying number of fragments. The algorithm aims to determine the size and the number if fragments. To determine the number of fragments in an image simple binary labeling algorithm is used. In order to count the number fragments, all image pixels are scanned and labels are assigned to nonzero pixels and recording label equivalences. Determine the equivalence classes and re label the pixels based on the classes resolved. The number of pixels that corresponds to DNA fragments is used to determine the fragment size by using the relation one pixel is equal to 263587.2 nanometer. The sizes of DNA fragments measured by the proposed method and Ficarra method are tabulated in Table.1

Table 1 : Measurement of DNA Fragments

DNA image	Ficarra Method [3]			Proposed Method		
	Total no of fragment	No of pixels	Size 10^6 nm	Total No of fragment	No of pixels	Size 10^6 nm
1	52	2741	722	22	2947	779
2	18	2511	661	217	3051	807
3	58	2550	674	44	3118	824
4	58	1450	383	40	2233	590
5	16	1682	445	19	1862	492
6	112	952	251	65	1377	364
7	125	2573	680	42	2726	721
8	31	1084	286	18	1173	310

In addition to real images, the algorithm has tested on computer-simulated AFM

Published By:
Blue Eyes Intelligence Engineering
& Sciences Publication (BEIESP)

Table II Performance Comparison

Input Fragment Size	FOM	TP	FN	FP	TN	TPR	FPR	TNR	ACC
	Ficarra Method								
15	0.4679	836	8112	2	41674	0.0934	4.7898	1.0000	0.8273
20	0.4619	1059	11941	5	37619	0.0815	1.3289	0.999	0.7442
25	0.4698	1042	13028	6	36548	0.0741	1.6414	0.9998	0.7227
30	0.4676	1139	14209	4	35272	0.0742	1.1339	0.9999	0.6996
35	0.4772	1425	15144	6	34034	0.0860	1.7619	0.9998	0.6810
40	0.4731	1763	20026	6	28829	0.0809	2.0808	0.9998	0.5770
	Proposed Method								
15	0.5647	624	8324	421	41255	0.0697	0.0101	0.9899	0.8397
20	0.5208	788	12212	739	36885	0.0606	0.0196	0.9804	0.7640
25	0.5933	927	13143	640	35914	0.0659	0.0175	0.9825	0.7425
30	0.5687	940	14408	880	34476	0.0612	0.0227	0.9973	0.7192
35	0.5792	1238	15331	86	33239	0.0747	0.0240	0.9760	0.7007
40	0.6036	1562	20227	1185	27650	0.0717	0.0411	0.9589	0.6043

DNA images. Images are simulated as prescribed in [1]. Six images with various numbers of fragments (i.e.) 15, 20, 25, 30, 35 and 40 with a size of [225 x 229] are generated as shown in Fig 6 and tested.

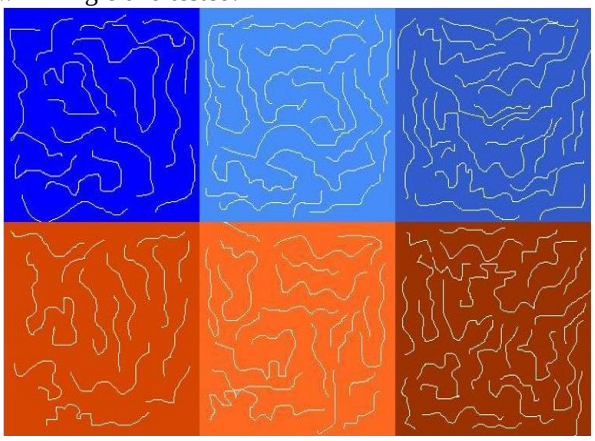

Figure 6 Computer Simulated Testing images:

Row 1- Fragments length of 15,20, and 25, Row 2- Fragments length of 30,35, and 40

The performances of proposed method and Ficarra method are compared. The parameters such as Figure of Merit (FOM) [16], true positive rate (RTP), false positive rate (RFP), accuracy (AC), specificity (SP) are used to evaluate the performances. The figure of merit is given by $\mathrm{FOM} = \frac{1}{[\max\{Ni,Nd\}]} \sum_{k=1}^{Nd} \frac{1}{1+\alpha d^2(k)}$, where N_i and N_d are the number of ideal and detected fragments, respectively, $d^2(k)$ distance between detected and ideal fragments and α is the scaling constant and is set to 1/9 in this experiment. The RTP or sensitivity is given by RTP = TP/ (TP+FN). RFP is defined as RFP= FP/(FP+TN). True negative rate (RTN) or Specificity is given by RTN=1-FP. Accuracy in percentage is obtained by AC= (TP+TN)/ (TP+TN+FP+FN) ×100 where TP - fragment in an image is detected correctly as fragment pixel, FP - Non-fragment pixel is detected wrongly as fragment pixel, TN-Non fragment pixel detected correctly as non-edge pixel, and FN- fragment pixel detected wrongly as non-edge pixel. The performances are evaluated using the above formulas and is tabulated in the Table II. It is observed that the accuracy, FOM of the proposed methodology is higher compared to the Ellisa method and also the sensitivity is low and the specificity and accuracy is high and provides better performance.

The error rate given by the proposed method is lower than the Ellisa method. A plot between length of fragments and error rate is shown in Fig 7. The fragment sizes are 583, 600, 602, 621, 663, and 694. The length of original image calculates their corresponding error rate.

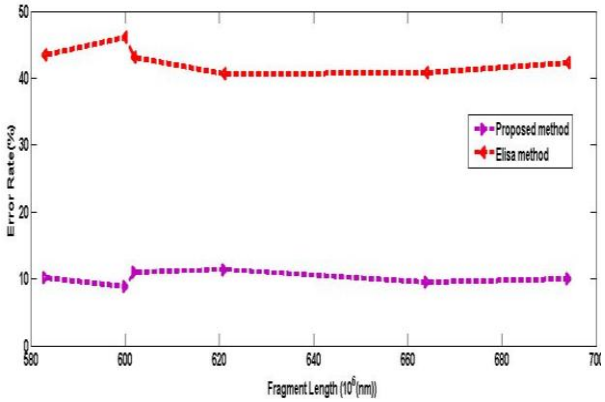

Figure 7: Fragment length vs error rate comparisons of proposed and existed method.

The performances of algorithm at various scales are tested. A plot between different scales and corresponding error rate is drawn. This graph shows the reason why the scale 4 is selected for our automated approach. The different scale levels (s1, s2, s3, s4) have been valued for the same image and their corresponding error rate is compared with that of original image. From the plot, the error rate decreases while we using more scales as shown in Fig 8. The error rate is computed by Error Rate (%) = [1 – ((length of fragmented image/length of simulated image)*100)].

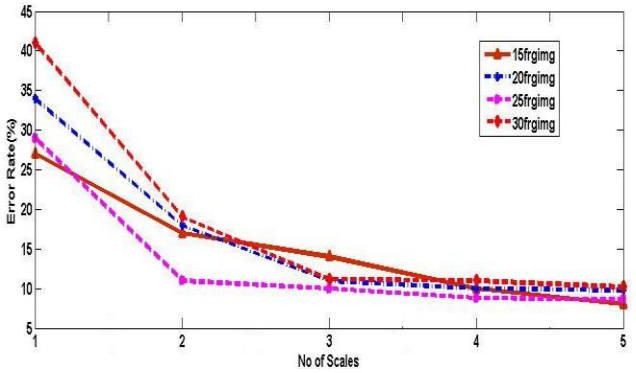

Figure 8: Scales vs error rate.

In order to test the algorithm at various noisy conditions, Gaussian noise of different levels say (0.01, 0.02, and 0.06) is added to the simulated image. It is seen that the while error rate increases with noise level. However, the proposed method is more robust than Ficarra [3].

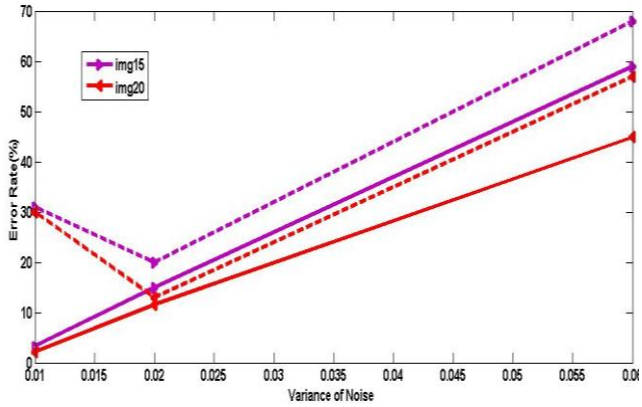

Figure 9: Noise vs error rate

The different noise variance [0.01, 0.02, 0.06], of '40 DNA fragment image' is tested with both algorithms and their corresponding error rate is plotted as in Fig 9.

I. CONCLUSION

Thus, an algorithm using wavelet transform for sizing the DNA molecule length in AFM images is presented and found to be effective. The proposed algorithm takes AFM images of DNA fragments as inputs, and elaborates them by a sequence of image processing steps in wavelet transform domain. The algorithm is tested using real and computer generated images. The DNA sizing of fragments is compared to already existing method. The improved performances are analyzed using Figure of Merit, accuracy, sensitivity, specificity, false positive rate. Moreover, the proposed algorithm proved its efficacy in various noise conditions.

REFERENCES

1. Rivetti, C., & Codeluppi, S. (2001). Accurate length determination of DNA molecules visualized by atomic force microscopy: evidence for a partial B-to A-form transition on mica. Ultramicroscopy, 87(1-2), 55-66.
2. Rivetti, C., Guthold, M., & Bustamante, C. (1999). Wrapping of DNA around the E. coli RNA polymerase open promoter complex. The EMBO journal, 18(16), 4464-4475.
3. Ficarra, E., Benini, L., Macii, E., & Zuccheri, G. (2005). Automated DNA fragments recognition and sizing through AFM image processing. IEEE Transactions on Information Technology in Biomedicine, 9(4), 508-517.
4. Meng, X., Benson, K., Chada, K., Huff, E. J., & Schwartz, D. C. (1995). Optical mapping of lambda bacteriophage clones using restriction endonucleases. Nature genetics, 9(4), 432.
5. Nie, S., & Zare, R. N. (1997). Optical detection of single molecules. Annual review of biophysics and biomolecular structure, 26(1), 567-596.
6. Ficarra, E., Masotti, D., Benini, L., Milano, M., & Bergia, A. (2002). Automated DNA curvature profile reconstruction in atomic force microscope images. AI* IA Notizie, 4, 64-68
7. Spisz, T. S., Fang, Y., Reeves, R. H., Seymour, C. K., Bankman, I. N., & Hoh, J. H. (1998). Automated sizing of DNA fragments in atomic force microscope images. Medical and Biological Engineering and Computing, 36(6), 667-672.ar
8. Sanchez-Sevilla, A., Thimonier, J., Marilley, M., Rocca-Serra, J., & Barbet, J. (2002). Accuracy of AFM measurements of the contour length of DNA fragments adsorbed on mica in air and in aqueous buffer. Ultramicroscopy, 92(3-4), 151-158.
9. Shao, Z., Mou, J., Czajkowsky, D. M., Yang, J., & Yuan, J. Y. (1996). Biological atomic force microscopy: what is achieved and what is needed. Advances in Physics, 45(1), 1-86.
10. Masotti, D., Ficarra, E., Macii, E., & Benini, L. (2004, May). Techniques for enhancing computation of DNA curvature molecules. In Bioinformatics and Bioengineering, 2004. BIBE 2004. Proceedings. Fourth IEEE Symposium on (pp. 22-29). IEEE
11. Chworos, A., & Obara, B. (2009). Automatic Analysis of Conjugated Polyelectrolyte–DNA Interactions Based on Sequential Analysis of AFM Imaging. IEEE Transactions on Nanotechnology, 8(4), 457-462.
12. Johnson, W.T., 2008. Imaging DNA in Solution with the AFM. Agilent Technologies, Oct.
13. Mallat, S. (2008). A wavelet tour of signal processing: the sparse way. Academic press.
14. Bao, Paul, and Lei Zhang. "Noise reduction for magnetic resonance images via adaptive multiscale products thresholding." IEEE transactions on medical imaging 22.9 (2003): 1089-1099.
15. Bao, P., Zhang, L., & Wu, X. (2005). Canny edge detection enhancement by scale multiplication. IEEE transactions on pattern analysis and machine intelligence, 27(9), 1485-1490.
16. Pratt, W. K. Digital Image Processing. 1991. Publisher John Wiley & Sons.

AUTHORS PROFILE

Anand.S received his B.E. Degree in Electronics and Communication Engineering in 1991, M.E degree in Communication Systems in 2002, and Ph.D degree in Medical Image Enhancement from Anna Universty Chennai. He is a life time member of ISTE, IETE, and ISCA. His current research interests include Antenna Design, and Image Processing. He had 25 years of teaching and research experience. Currently he is working as Professor, Electronics and Communication Engineering, Mepco Schlenk Engineering College, Sivakasi, Tamil Nadu, India. He has publshed more than 100 research atrticles in reputed journals and conferences. He reviewed various papers for Elsevier, Springer, and Wiley publications.

Lakshmanan B completed his B.Tech Degree in Information Technology in 2008, M.Tech Degree in Information Technology in 2010 and currently pursuing PhD in the area of Medical Image processing. He has undergone two month IASc Research Fellowship at Soft Computing Research Centre (ISI) and worked under the guidance of Prof.Sankar K Pal,Distinguished Scientist & Former Director of Indian Statistical Institute, Kolkata.

Published By:
Blue Eyes Intelligence Engineering
& Sciences Publication (BEIESP)

His area of interest include Machine Intelligence, Deep Learning, Medical Imaging and Data Mining.He has got nine years of teaching experience. He has authored or coauthored about 12 publications in journal/conference level.He is currently working as Assistant Professor(Senior Grade) in the Department of Computer Science and Engineering,Mepco Schlenk Engineering College,Sivakasi,Tamilnadu,India and he is a Life Member of Indian Society of Technical Education(ISTE) and Computer Society of India(CSI).

Valarmathi received her B.E. degree in Computer Engineering in 1990 and M.E. degree in Embedded System Technologies in 2010. Currently, she is pursuing Ph.D degree at Anna University, Chennai. Currently, she is working as an Senior Grade Lecturer in the Department of Electronics and Communication Engineering at Virudhunagar S.Vellaichamy Nadar Polytechnicn College, Virudhunagar, Tamilnadu, India. Her research interest includes Image Contrast Enhancement**.**

Kavitha Nagarathinam graduated B.E.,(IT) from Bharathidasan University in the year 2004 and M.E.,(CSE) from Anna University, Chennai, in the year 2006**.** She is currently associated with Saranathan College of Engineering, Trichy, Tamil Nadu, India as an Assistant Professor and has 10 years of teaching experience in various subjects in the field of Computer Science. She is currently pursuing PhD in the area of Image and Video Processing, Artificial Intelligence. She has published more than 10 research articles in various reputed Journals and Conferences.